

Pathological mineralization of calcium phosphate

Mineralización patológica de fosfato cálcico

Félix Grases¹, Otakar Sohnel²

1. Laboratory of Renal Lithiasis Research, University Institute of Health Sciences Research (IUNICS),
University of Balearic Islands, Palma de Mallorca, Spain

2. University of J.E. Purkyně, Faculty of Environmental Studies, Ústí n.L., Czech Republic

Correspondencia

Félix Grases Freixedas

Instituto Universitario de Investigación en Ciencias de la Salud (IUNICS)

Universidad de las Islas Baleares. Ctra. Valldemossa km 7,5

07122 - Palma de Mallorca

E-mail: fgrases@uib.es

Recibido: 21 - I - 2015

Aceptado: 29 - I - 2015

doi: 10.3306/MEDICINABALEAR.30.01.43

Abstract

Based on the study of non-infected calcium phosphate renal calculi, solid concretions formed in simulated body fluid and calcific deposits formed in human aortic valves, two different mechanisms of hydroxyapatite (HAP) formation are described. In a mechanism, the formation of spherical HAP particles takes place via aggregation of Posner's clusters present in the liquid, after reaching a certain size gradually settled in the liquid and became incorporated into developing concretion. In the other mechanism, the microcolumnar HAP crystals were nucleated on randomly distributed detritus of organic origin embedded in the compact phase.

Keywords: Biological hydroxyapatite, formation mechanism, renal calculi, aortic valve, body fluid

Resumen

Basándonos en estudios de los cálculos renales no infecciosos, concreciones sólidas obtenidas *in vitro* utilizando fluidos biológicos simulados y depósitos calcificados formados en válvulas aórticas humanas, se describen dos mecanismos diferentes que explican el desarrollo de la hidroxapatita (HAP). En uno de los mecanismos, la formación de nanopartículas esféricas de HAP tiene lugar a través de la agregación de macroespecies de Posner presentes en el líquido, que a su vez se agrupan mediante nucleación superficial formando concreciones de mayor tamaño. En el otro mecanismo, la formación de cristales microcolumnares de HAP tiene lugar mediante procesos de nucleación heterogénea sobre detritus de materia orgánica localizados en espacios confinados y poco irrigados.

Palabras clave: Hidroxapatita biológica, mecanismo de formación, cálculo renal, válvula aórtica, fluido biológico

Pathologic mineralization is defined as the deposition of primarily phosphatic and calcium oxalate minerals from body fluids, including blood, plasma, interstitial fluid, urine and saliva, on undesired sites such as the aortic valve, kidneys, arteries and veins. Although the etiology of mineralization has been studied for nearly a century, not all aspects of this process are fully understood.

It is generally agreed that the formation and deposition of minerals from body fluids can occur only when the fluid is supersaturated with that mineral. As body fluids are frequently supersaturated, other conditions, such as deficiencies in specific inhibitors, the presence of nucleation substrates and abnormally high concentration of specific

ions, must also be present to facilitate the formation and deposition of minerals.

Heterogeneous nucleation of a solid on an appropriate substrate followed by classical crystallization route, i.e. incorporation of individual building units – ions - represents a commonly accepted concept formation and development of solid deposits. Arrival of ions to the binding site is governed by volume and/or surface diffusion. Crystals with well-developed habitus originate in a slightly supersaturated fluid, whereas shapeless, often amorphous, solids can be formed from highly supersaturated liquid. Calculations have shown, however, that the classical crystallization mechanism is highly questionable in the

case of hydroxyapatite (hereafter HAP), since the probability of incorporation of growth units into the bulk crystal is extremely low¹.

A different mechanism of HAP crystal growth is based on the concept of pre-nucleation clusters that form in supersaturated solutions¹⁰. Specifically, Posner's clusters form in liquids supersaturated with respect to HAP^{1,2}. The presence of these clusters with assumed composition $\text{Ca}_9(\text{PO}_4)_6$ and about 1 nm in diameter was observed in a solution just saturated with HAP^{1,3} and was recently confirmed experimentally in simulated body fluid⁴. According to this mechanism the growth of HAP crystals proceeds by direct incorporation of agglomerates of Posner's clusters, not individual ions, into the bulk crystal.

The formation of spherical HAP particles via Posner's clusters was experimentally found to proceed in 5 stages: **1)** coagulation of calcium phosphate clusters 1 nm in diameter into larger entities, **2)** accretion of these entities into agglomerates, **3)** formation of domains of closely associated agglomerates about 50 nm in diameter, **4)** transformation of domains into amorphous spherical particles about 150 nm in diameter, and **5)** formation of spherical objects with an average diameter of 10-30 μm coexisting with remaining domains. This mechanism, specifically phases **3)** to **5)**, is active when suitable organic substrate is present^{5,6}.

Amorphous matter can be gradually transformed into crystalline matter by solution-mediated or solid state aging. Solution-mediated transformation involves the slow dissolution of amorphous matter in a surrounding liquid and its gradual deposition onto a surface nucleus (nuclei). Thus, the transformation of a shapeless amorphous solid results in the formation of crystal(s) bounded

by flat faces, i.e. the habitus of newly formed crystals adopts a nearly or fully equilibrated shape. In contrast, solid state transformation proceeds through changes in the internal structure of a solid without contact with a liquid resulting in the formation of a crystalline lattice from amorphous matter without a change in the external shape of the particle, i.e. the original shape of particle remains unchanged.

Phosphate renal calculi are formed in the kidney cavity with poor urodynamics, i.e. in a cavity of the kidney in which the average residence time of largely stagnant urine substantially exceeds that of urine in the kidney pelvis. An adequate volume of urine is retained in this cavity. A phosphate calculus that forms in the kidney cavity is composed of a structureless compact phosphatic phase in the form of layers and blocks, abundant organic matter and large spherules disseminated throughout the calculus volume or occurring in large and often intergrown assemblies^{5,6}. AFM showed that the compact phase consists of two distinctly different morphological forms of the phosphatic phase: a predominant phase consisting of spherical agglomerates with diameters up to 300 nm made up of spherulites of approximately 10 nm in diameter, and a less common phase consisting of separate and/or intergrown columnar crystals disseminated without any apparent order in the calculus interior **Figure 1, 2**⁷.

Solid concretions originating in 50 ml of stagnant simulated body fluid on a polymeric substrate situated on the bottom of an experimental vessel consisted of agglomerates 30 to 120 nm in diameter, but no crystals, **Figure 3**⁸. If the polymeric substrate had been positioned vertically, however, only a few hemispheres would have formed. The mechanical properties of the material forming the hemispheres were identical, indicating that the chemical compo-

Figure 1: AFM 3-D topographic image of the cross-section of the compact phase of the non-infectious phosphatic renal stone. Scan (a) 20 x 20 μm , (b) 3.3 x 3.3 μm . The red and yellow regions correspond to depressions, i.e. sites situated below the plane of the surface, and projections from the surface, respectively. Columnar crystals are indicated by arrows; surface is composed of agglomerates.

Figure 1a

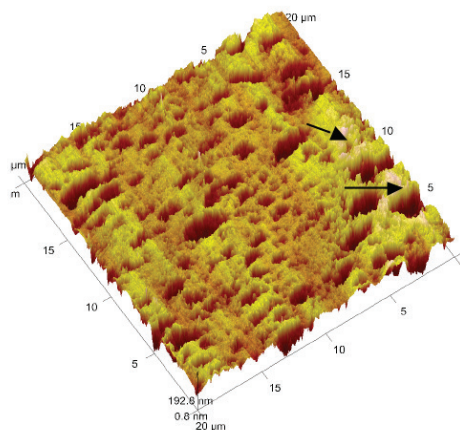
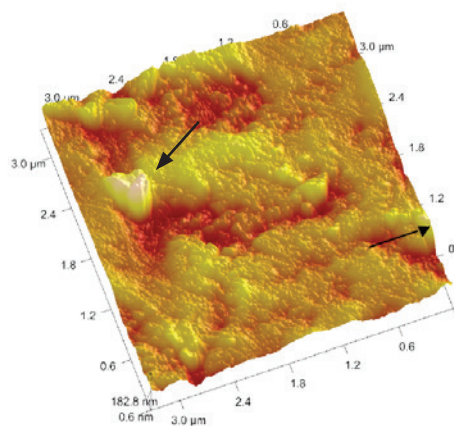


Figure 1b



sition was uniform. The hemispheres were composed of amorphous material without any sign of crystallinity.

The structure of phosphate deposits formed in the human aortic valve differs from the structure of the urinary and synthetic concretions described above. The former deposits were formed by blocks of closely arranged elongated needle- and plate-like crystals and irregularly disseminated areas of soft organic material, **Figure 4**⁹. Any sporadically present large cavities containing small spherical objects were formed either by the irregular growth of individual blocks of the compact phosphatic phase or by intergrowth of two deposits developing in close vicinity.

These observations indicate that the structure of pathological deposits of calcium phosphate is influenced both by the volume of fluid from which the deposit forms and by the spatial orientation of the substrate on which the deposit forms.

In an adequate volume of body fluid in which uroliths and synthetic hemispheres form, the cluster mechanism predominates and the deposits are primarily composed of agglomerates of amorphous calcium phosphate. In contrast, aortic deposits originate in a confined space with their surface just wetted by a thin and nearly stagnant laminar layer of liquid. Although Posner's clusters must also be present in this layer of liquid, the spatial limitations restrict the formation of bigger agglomerates and the deposits grow via the classical crystallization route, i.e. by incorporation of building units, probably Posner's clusters, into the bulk of the deposit.

The spatial orientation of substrate also plays a role in deposit formation. If the substrate is oriented horizontally,

the number of particles arriving on the surface of substrate due to Brownian motion is augmented by settling of large agglomerates in the gravitational field. If the substrate is oriented vertically, then particles arrive on the surface only due to Brownian motion. Therefore, greater number of particles arrives on the surface of horizontally than on vertically oriented substrate in the same period of time.

The effect of settling on the deposit development can be estimated as follows:

The settling velocity of particles, v , in a stagnant liquid can be calculated from Stokes law if Reynolds number Re of the particle is less than 0.1

$$v = 2(\rho - \rho_0) r^2 g / 9 \eta_0 \quad (1)$$

where ρ and ρ_0 is the density of the particle and liquid respectively, r is the radius of the particle, g is the acceleration due to gravity and η_0 is the dynamic viscosity of the liquid. Using values $\rho = 3160 \text{ kg.m}^{-3}$, $\rho_0 = 1020 \text{ kg.m}^{-3}$ (plasma density at 37°C¹²) and $\eta_0 = 1.39 \times 10^{-3} \text{ Pa.s}$ (plasma viscosity at 37°C¹¹), $r = 5 \times 10^{-8} \text{ m}$, $g = 9.81 \text{ m.s}^{-2}$ the settling velocity is $8.4 \times 10^{-9} \text{ m.s}^{-1}$, i.e. $3.02 \times 10^{-5} \text{ m/hr}$.

The particle Reynolds number for a sphere in a fluid is defined as

$$Re = \rho v L / \eta \quad (2)$$

where L is the characteristic dimension of the particle (diameter in case of sphere). For the cluster considered above $Re = 9 \times 10^{-10}$. Hence, eq. (1) is applicable in our case.

Figure 2: AFM nanoscale modulus map of the cross-section of the compact phase of the non-infectious phosphatic stone. Diameter of individual particles is about 10 nm. Red and yellow colours indicate sites composed of soft organic matter and stiff inorganic matter, respectively.

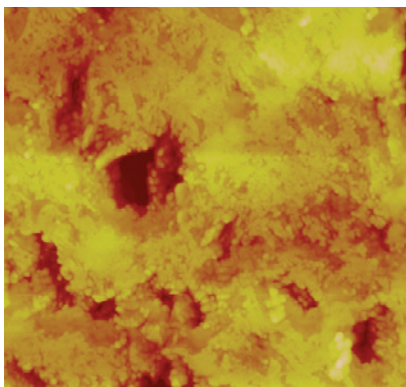


Figure 3: AFM 3-D topographic image of the cross-section of surface layer of synthetic hemisphere. Scan $8 \times 8 \mu\text{m}$. Light yellow colour indicates stiff material. This layer composed of agglomerates contains no crystals. Red parts of the image is organic matter in which synthetic hemisphere is fixed.

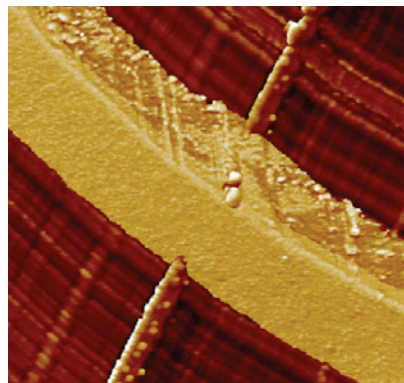
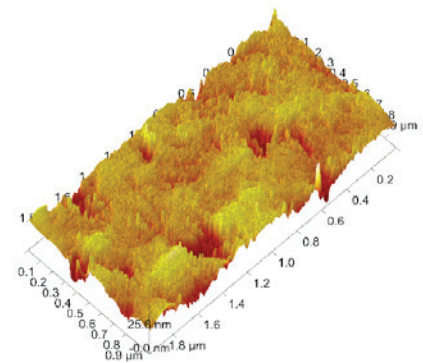


Figure 4: AFM 3-D topographic image of the cross-section of aortic valve deposit. Scan $1 \times 2 \mu\text{m}$. Attached needle- and plate-like crystals from the cross-section; agglomerates are not present.



The number of particles arriving on a substrate surface due to Brownian motion can be estimated from the mean displacement of particle in one direction Δx ¹³

$$\Delta x = [(R T t) / (3 \pi N A r \eta_0)]^{1/2} \quad (3)$$

where R is the universal gas constant 8.31 J/K mol, T is temperature in K, t is time in seconds, NA is Avogadro's number 6.022×10^{23} /mol, r is the radius of particle in meters and η_0 is the viscosity 1.39×10^{-3} Pa s. According to eq.(3), the mean displacement of aggregate 100 nm in diameter from eq. (3) is 9×10^{-5} m/hr.

Particles move due to Brownian motion in all directions. Assuming that movement occurs just in the directions of the Cartesian axes, then only one-sixth of the particles present would move towards the substrate. This is, one-sixth of the agglomerates of radius 50 nm present in a 90 μm layer of stagnant liquid adjoining the substrate will reach its surface. When settling is also effective, then all agglomerates within 30 μm from the surface and one-sixth of the particles present in the liquid layer located 30 to 90 μm from the surface will reach the substrate. Thus, 2.5-fold more agglomerates of radius of 50 nm will

reach the surface of a horizontally situated substrate than a vertically situated surface during the same period of time. For agglomerates of radius 25 nm this difference is 1.3-fold.

The following mechanism of the formation of both types of concretions was hypothesized based on their ultra-fine structure: spherical agglomerates that formed via aggregation of Posner's clusters present in liquid, i.e. urine and simulated body fluid, after reaching a certain size gradually settled in the liquid and became incorporated into developing concretion. The columnar crystals irregularly disseminated in a phosphate calculus were nucleated on randomly distributed detritus of organic origin embedded in the compact phase. In both cases the settling of agglomerates onto concretions was found to be the principal mechanism of their formation from stagnant liquid in cavities of low urodynamic efficacy.

Conflict of interest

The authors declare that they have no competing interests

References

1. Onuma K, Ito A. Cluster growth model for hydroxyapatite. *Chem Mater*. 1998; 10:3346-3351.
2. Posner AS, Betts F. Synthetic amorphous calcium phosphate and its relation to bone mineral structure. *Acc Chem Res* 1975; 8:273-281.
3. Oyane A, Onuma K, Kokubo T, Ito A. Clustering of calcium phosphate in the system $\text{CaCl}_2\text{-H}_3\text{PO}_4\text{-KCl-H}_2\text{O}$. *J Phys Chem B* 1999; 15:6557-6562.
4. Dey A, Bomans PHH, Muller F, Will J, Frederik PM, de With G, Somerdijk AJM. The role of prenucleation clusters in surface-induced calcium phosphate crystallization. *Nature Materials*. 2010; 9: 1010-1014.
5. Grases F, Costa-Bauzá A, Prieto RM, Gomila I, Pieras E, Söhnel O. Non-infectious phosphate renal calculi: Fine structure, chemical and phase composition. *Scand J Clin Lab Invest*. 2011;00:1-6.
6. Grases F, Söhnel O, Vilacampa AI, March JG. Phosphates precipitating from artificial urine and fine structure of phosphate renal calculi. *Clin Chim Acta*. 1996; 244: 45-67.
7. Zelenková M, Söhnel O, Grases F. Ultrafine structure of the hydroxyapatite amorphous phase in non-infectious phosphate renal calculi. *Urology* 2012, 79(4) 968.e1-6.
8. Grases F, Zelenková M, Söhnel O. Structure and formation of calcium phosphate concretions formed in simulated body fluid. *Urolithiasis* 2014, (42): 9-16.
9. Grases F, Söhnel O, Zelenková M. Ultrafine structure of human aortic valve calcific deposits. *J Citol Histol*. 2014, (5) 214, doi:10.4172/2157-7099.1000214.
10. Mullin JW, Leci CL. Evidence of molecular cluster formation in supersaturated solutions of citric acid. *Philosophical Magazine* 1969, 19(161):1075-77.
11. Rosenson RS, McCormick A, Uretz EF. Distribution of blood viscosity values and biochemical correlates in healthy adults. *Clinical Chem*. 1996, 42(8):1189-1195.
12. Trudnowski RJ, Rico RC. Specific Gravity of Blood and Plasma at 4 and 37 °C. *Clinical Chem*. 1994, 20(5):615-616.